NUMERICAL SIMULATION OF THREE-DIMENSIONAL SHOCK-WAVE/BOUNDARY-LAYER INTERACTION ON SHARP AND BLUNTED FLAT PLATE

V. Borovoy, I. Egorov, D. Ivanov
Central Aerohydrodynamic Institute (TsAGI)
volf.borovoy@gmail.com; ivan.egorov@tsagi.ru

Abstract

Interaction of shock waves with turbulent boundary layer and laminar boundary layer is investigated. Numerical investigation of gas flow on a flat plate near a single fin and a fin pair, generating crossings shocks, is performed at Mach numbers $M_\infty = 5$ ($Re_{\infty L} = 27\times10^6$) u $M_\infty = 6$ ($Re_{\infty L} = 19\times10^6$). The study is focused upon the plate bluntness influence on the flow field and heat transfer in the interaction region.

1 Introduction

A great number of works (for-example [1-2]) are dedicated to the investigation of interaction of the oblique shock waves, generated by a single fin or a fin pair, with boundary layer of the plate on which they are installed. Firstly, experimental investigations were carried out. During last two decades, high attention has been also paid to the numerical simulation of such flows. The review of the experimental and computational works performed up to 2003 is presented in [2].

Almost in all the works, the interference flow on the sharp plate is studied. At the same time, the investigations of two-dimensional interference between an oblique shock wave and laminar boundary layer of the plate [3] show that even a small bluntness of the plate leading edge significantly decreases heat exchange in the shock incidence region. It also turns out that there is a threshold value of the plate blunting radius [4]: the maximum heat transfer coefficient significantly decreases as the radius increases only up to a certain threshold value; the further blunting slightly influences on the maximum value of the heat-transfer coefficient. These peculiarities are related to the influence of the high-entropy layer, generated by the blunted leading edge, on the flow in the separation zone, caused by the incident shock wave.

In the present work, interaction of shock waves with turbulent boundary layer and laminar boundary layer is investigated. Numerical investigation of gas flow on a flat plate near a single fin and a fin pair, generating crossings shocks, is performed. The study is focused upon the plate bluntness influence on the flow field and heat transfer in the interaction region. The numerical calculations were carried out at Mach numbers M=5, 6 and 8 and Reynolds numbers $Re_{\infty L}$ up to 27×10^6. For numerical flow simulation, the three-dimensional Reynolds-averaged Navier-Stokes equations are solved, using the q-ω turbulence model.

It is established that even small plate blunting significantly influences on heat transfer and pressure distributions. Moreover in some cases, it can cause global transformation of the flow structure in the area of interference between the shock waves and boundary layer.

2 The model and experimental investigation

The main part of models is a plate of length L = 319 mm and width W = 150 mm (Fig.1)

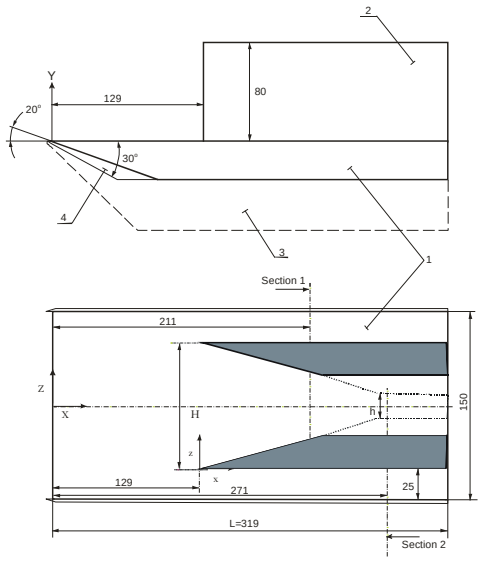

Fig. 1. Scheme of models: 1 – plate, 2 – wedges, 3 – lateral joint bars, 4 – front joint bar.

Sharp wedge 2 is set on the plate. Its leading edge is located at distance X_o = 129 mm from narrow leading edge of the plate. Wedges with angles of flow angularity θ = 10°, 15° и 20° are tested. Wedge thickness is b = 25 or 37.5 mm. On the plate removable front joint bars 3 are fixed, which are used for variation of leading edge blunting radius. Furthermore, lateral joint bars 4 are fixed on the plate, which are attenuate gas flow from one surface to another one.

Experiments were carried out in TsAGI shock tube UT-1M. The tube worked on Ludwig tube scheme. Duration of steady flow is 40 ms. Shaped nozzles with diameter of output cross-section 300 mm were used. Characteristics of undisturbed flow are presented in table 1.

Table 1

Mach number M_∞	Total pressure P_o, bar	Total temperature T_o, K	Reynolds number $Re_{\infty L}$
5	69	530	$27x10^6$
6	90	560	$19x10^6$

At Mach number M_∞ = 5 at some distance from leading edge of the plate natural laminar-turbulent transition of boundary layer occurs. At M∞ = 6 turbulator is used, situated at distance 20 mm from leading edge of the plate. It represents 3 rows of cylinders, having 1mm diameter, 0.2 mm height with 1mm interval along the edge. Boundary layer transits to turbulent state directly behind the turbulator.

Luminescent temperature converters Ref. [5] and heat flux thermocouple sensors kind of "thin wall" Ref. [6] are used to investigate heat transfer, and luminescent pressure converters Ref. [5] are used to investigate pressure distribution. Gas flow near plate surface is visualized using method, recently developed in TsAGI Ref. [7]. It is based on measurements of small oil displacements, marked by contrast luminescent particles

3 Numerical simulation

Numerical simulation of flow is implemented by solving Reynolds-averaged Navier-Stokes equations, closed by q – ω turbulence model, following turbulence characteristics are assumed: free stream turbulence, referred to free stream velocity - q = 0.01, frequency of turbulent pulsations, referred to characteristic time ω = 1. Experimental data given below indicate that flow in region, located before the wedge, (in region 1, $X<X_o$) practically doesn't depend on flow in the vicinity of the wedge (in region 2, $X>X_o$), flow in region 1 – simply two-dimensional flow over the plate, and it may be calculated regardless of region 2, what allows to save computational resources. Having computed flow over the plate, length of which is slightly greater, than X_o, we obtain velocity, pressure and temperature profiles in section $X = X_o$. These data are used as inlet boundary condition for region 2. In region 1 simple two-dimensional grid is used. In region 2 three-dimensional single-block grid of dimension 81x71x61 nodes is generated. For this region following boundaries are chosen: towards z axis – from the wedge surface to the middle of the plate, and towards x axis – from leading edge of the wedge to the end of the plate. Grids are quasi-orthogonal and generated using integral method, based on numerical implementation of conformal transformation Ref. [8]. To resolve laminar and turbulent boundary layers on the wedge and the plate, nodes of computational grid are clustered close by solid surface, quasi-

one-dimensional algorithm is used, based on algebraic transformation. On grid clustering close by solid surface three zones of thickness Re^{-1}, $2\,\mathrm{Re}^{-1/2}$ и $1.5\,\mathrm{Re}^{-1/5}$ are selected. Every such zone contains 6, 15 and 20% of total number of nodes in direction, normal to solid surface. Detailed description of the method is given in [9].

4 Results of investigation

In Fig.2 results of optical investigations of flow characteristics near surface of sharp plate (r = 0) and weakly blunt plate (r = 0.75 mm, $r/X_o = 0.0058$) at Mach number $M_\infty = 5$ and Reynolds number $\mathrm{Re}_{\infty L} = 27 \times 10^6$ are given as an example. On the plate sharp wedge with angle $\theta = 15°$ is set. In Fig. 2,a lines of constant values of Stanton number are shown:

$$St = q/\rho_\infty U_\infty c_p(T_o - T_w).$$

Here q – measured heat flux, ρ_∞ and U_∞ - density and velocity of gas in undisturbed flow, T_o – total temperature. Generation of turbulent wedges is seen. They are begin near leading edge of the plate, both sharp and blunt. Their location doesn't depend on bluntness size, and they are generated under the influence of disturbances, coming from the nozzle. Laminar-turbulent transition ends at some distance from leading edge, where turbulent wedges close in. Plate leading edge bluntness up to 0.5 mm displaces transition line downstream, and further plate bluntness displaces it upstream. At r = 0.5 mm laminar-turbulent transition ends behind leading edge of the wedge; close to leading edge of the wedge oblique shock interacts with transitional boundary layer. At another values of bluntness radius oblique shock, generated by the wedge, interacts with turbulent boundary layer.

In Fig. 2, b lines of constant values of pressure coefficient Cp are shown:

$$Cp = (P - P_\infty)/1/2\ \rho_\infty U_\infty^2$$

In Fig.2, c threshold streamlines on the plate surface are given. Generation of separation line before shock and attachment line behind it is seen. Unfortunately, out of interference region, where friction stresses are small, shape and direction of streamlines are distorted because of influence of inertial forces, caused by the model vibrations. Figure 2,c also gives qualitative idea of friction stresses: the more blackening extent of the image, the more friction stress. Value of friction stress is estimated using measured displacement of solid particles, included in oil, over definite time interval. It is seen that distribution of friction stresses agrees with distribution of heat-transfer coefficient. In particular, location and shape of laminar-turbulent transition lines, determined using heat-transfer and friction coefficient distributions, are close to each other.

Figure 2 shows that in the vicinity of the attachment line values of heat flux, pressure and friction dramatically increase. From comparison of experimental data for sharp and blunt plates it follows that plate bluntness reduces levels of maximum heat exchange and maximum pressure in region of shock interference with boundary layer. However, interference region slightly expands. Plate bluntness also leads to extension of initial interference zone. Results, presented below, give quantitative information about it.

r = 0 r = 0.75 mm

a

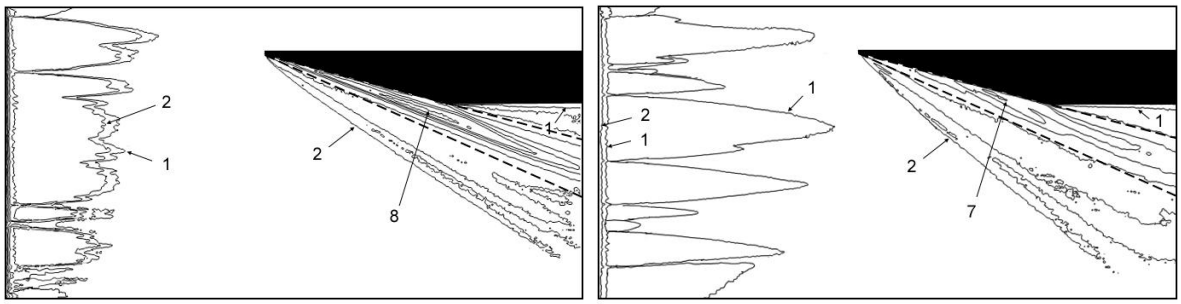

b

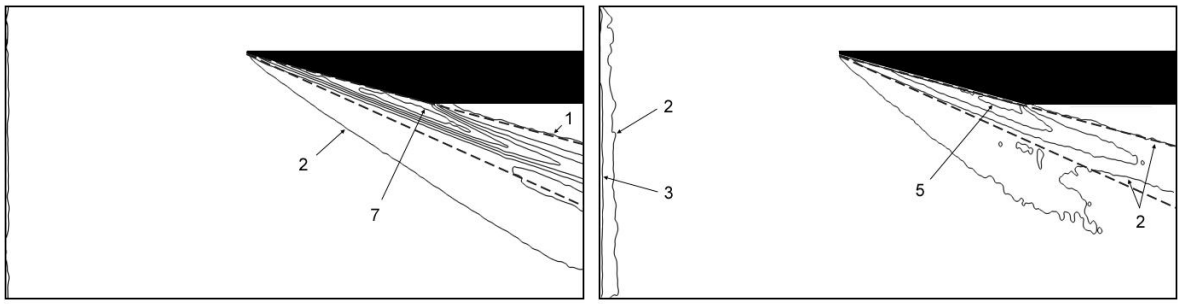

c

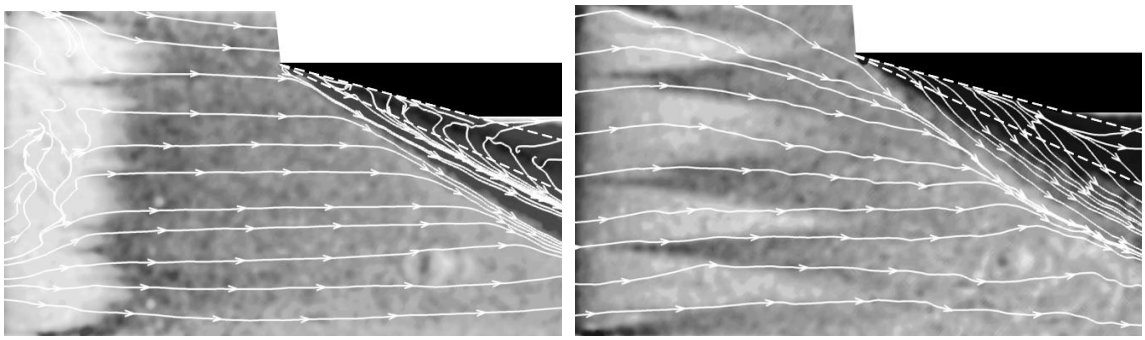

Fig. 2. Gas flow on the plate with wedge $\theta = 15^o$ at M = 5 and $Re_{\infty L} = 27x10^6$: on the left – sharp plate (r = 0), on the right – blunted plate (r = 0.75 mm, $r/X_o = 5.8x10^{-3}$). a) Stanton number (1 – St = 0.0002; 2 - 0.0003; 3 - 0.0004; 4 - 0.0006; 5 - 0.0010; 6 - 0.0014; 7 - 0.0018; 8 - 0.0022), b) pressure coefficient (1 – Cp = 0; 2 - 0.045; 3 - 0.090; 4 - 0.135; 5 - 0.180, 6 - 0.225; 7 - 0.270), c) Threshold streamlines. Dashed lines show location of shock (in two-dimensional flow of inviscid gas) и attachment lines.

Maximum Stanton numbers St_m at various distances x from leading edge of the wedge are determined using Stanton number measurements with help of luminescent coating. In Fig.3 these values are given as an example for angle $\theta = 10°$, depending on x/X_o, where x – distance from the wedge leading edge, and X_o = 129mm – coordinate of the wedge leading edge (Fig. 1). It is seen that at M = 5 and $Re_{\infty L} = 27\times10^6$ initial region of interference zone, i.e. region, where variable St_m significantly changes, has considerable length: near the wedge with angle $\theta = 10°$ relative length of this zone x/X_o is approximately equal to 0.5 on sharp plate and $x/X_o \approx 0.8$ at bluntness radius r = 0.75 mm. At $\theta = 15°$ length of initial region is less, than at $\theta = 10°$. At $\theta = 20°$ initial interference region occupies on sharp plate all wedge length up to corner; it occurs because of the fact that the wedge length at $\theta = 20°$

($x/X_o = 0.53$) is less, than at $\theta = 10°$ and 15°, as all wedges, used in optical measurements, have the same thickness b = 25 mm, Fig.1. In initial zone not only heat-transfer coefficient significantly increases along the wedge, but also pressure coefficient.

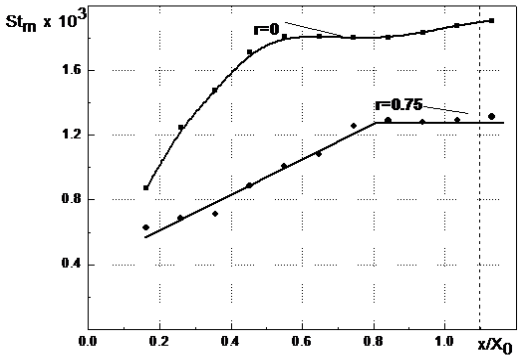

Fig. 3. Lenghtwise distribution of maximum values of Stanton number St_m close to wedge with angle $\theta = 10°$ at M=5 and $Re_{\infty L} = 27 \times 10^6$.

For two values of plate bluntness radius (r = 0 и 0.75 mm) numerical simulation of flow at M = 5, $Re_{\infty L} = 27 \times 10^6$ is fulfilled. Reynolds-averaged Navier-Stokes equations are solving with use of q-ω model turbulence model ref. [9]. In Fig. 4 results of Stanton number calculation are compared with results of measurements, fulfilled using luminescent coating and thermocouples. At turbulence parameters and value of inflow turbulence chosen numerical results satisfactory agree with experimental data, computational data closer to readings of thermocouple sensors, which are slightly more accurate, than optical measurements.

In Fig.5 results of maximum Stanton number St_m and pressure coefficient Cp_m measurements in section $x/X_o = 0.64$ at various wedge angles are presented versus ξ, where $\xi = P_2/P_1$ - ratio of pressure behind shock to pressure before it in inviscid flow. Value St_m is related to value of Stanton number, calculated for sharp plate at the same section in turbulent flow Ref. [10], and pressure P_m is related to pressure in undisturbed flow ($P_1 = P_\infty$). Heat-transfer coefficient is measured by thermocouples near thickened wedges (b = 37.5 mm), and pressure – using luminescent coating near wedges of thickness 25 mm. For sharp plate results of the work agree with results of work [2] (in [2] measurements are carried out in several cross sections at $x/X_o \geq 0.3$). Discrepancies are approximately 15%. They are specified by: a) measurement inaccuracy, b) slight differences in conditions of flow over models, c) difference in methods of undisturbed values determination (in [2] St_o and P_1 are determined experimentally, and in this work - numerically).

Figure 5 shows that plate bluntness significantly reduces maximum values of Stanton number and pressure at all investigated intensities of shock, generated by the wedge. As ξ increases, ratios St_m/St_o and P_m/P_1 steadily increase (at bluntness radius r = 2 mm relation St_m/St_o increases approximately proportionally to $\xi^{0.8}$). Regular character of heat transfer and pressure coefficient change versus ξ disturbs at maximum shock intensity (at $\theta = 20^o$) and large plate bluntness. It happens because of the fact that under the circumstances, as stated above, section I is located in initial interaction region, where values of heat transfer and pressure coefficients are less, than in quasi-conical region. In Fig.6 dependence of ratio St_m/St_{ms} on plate bluntness radius at $M_\infty = 6$ and $Re_{\infty L} = 19 \times 10^6$ is presented (luminescent coating is used). In the work turbulator is set on the plate, and laminar-turbulent transition takes place close to plate leading edge. In work [5] similar experiments are carried out without turbulator, and boundary layer is in transient state before the shock. Results of both cycles of experiments are close to each other, i.e. at transient and turbulent states of boundary layer plate bluntness gives rise to approximately equal weakening of heat transfer in zone of shock incidence. At $M_\infty = 6$, as at $M_\infty = 5$, bluntness increase at $r/X_o > 0.015$ slightly influences on value of the maximum heat transfer coefficient.

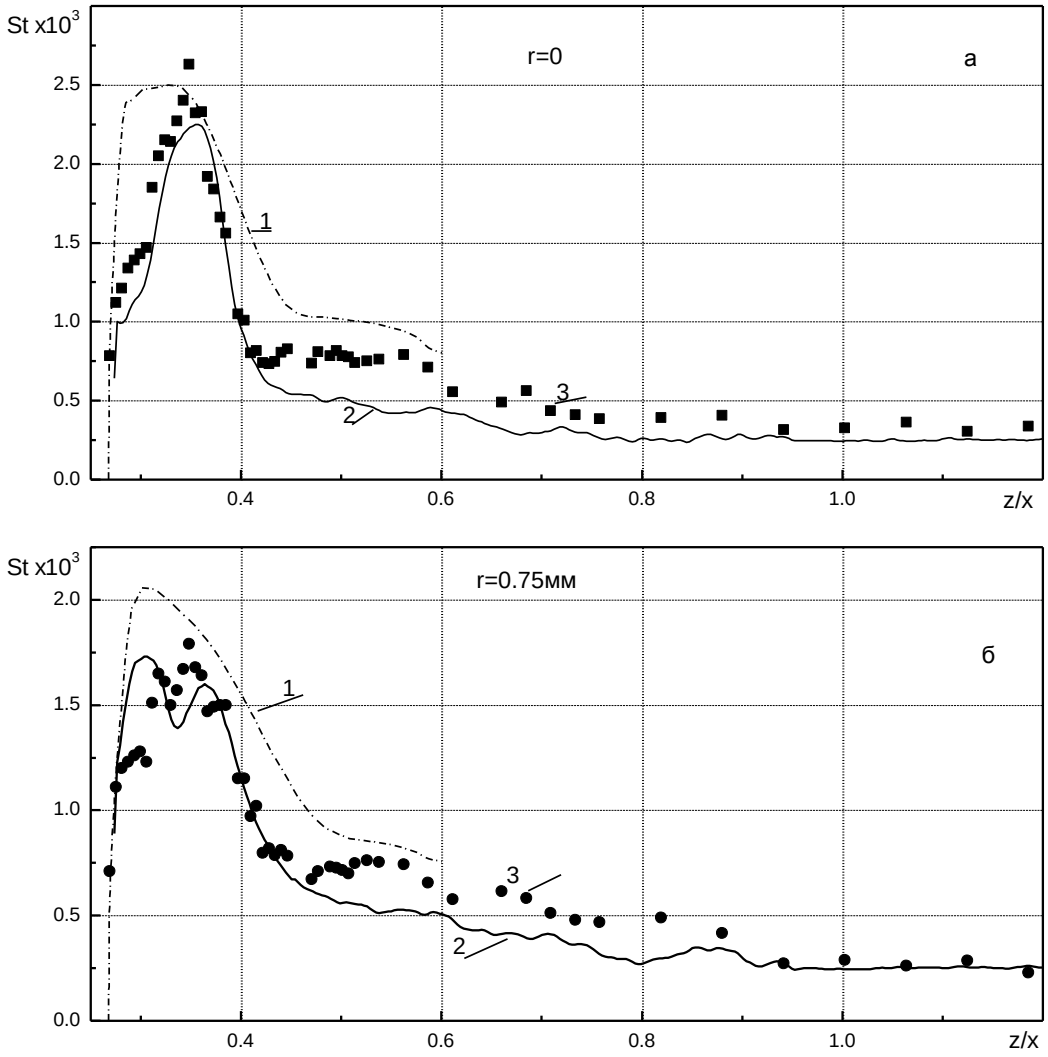

Fig. 4. Comparison of computational results with results of heat transfer coefficient measurements in section I ($X = 211$ mm, $x/X_o = 0.64$) at $M = 5$, $Re_{\infty L} = 27 \times 10^6$ and $\theta = 15^o$: a – r = 0, b – r = 0.75 mm, 1 – calculations, 2 – luminescent coating, 3 – thermocouples.

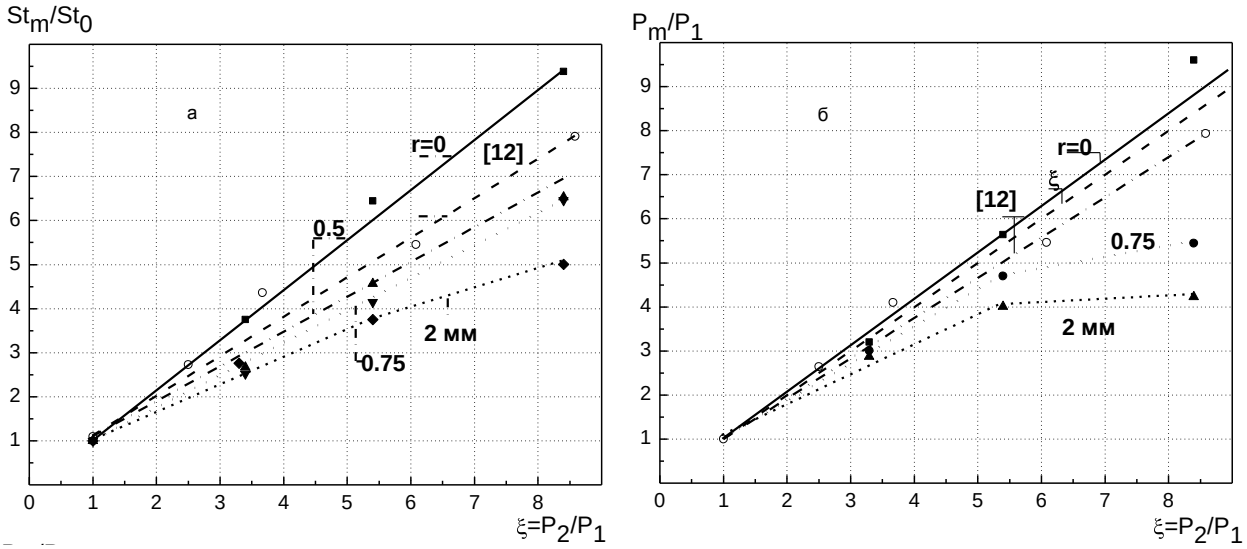

Fig. 5. Maximum heat exchenge enhancement St_m/St_o and maximum pressure increase P_m/P_1 in cross section I ($x/X_o = 0.64$) at M = 5 versus calculation extent of pressure increase ξ in oblique shock.

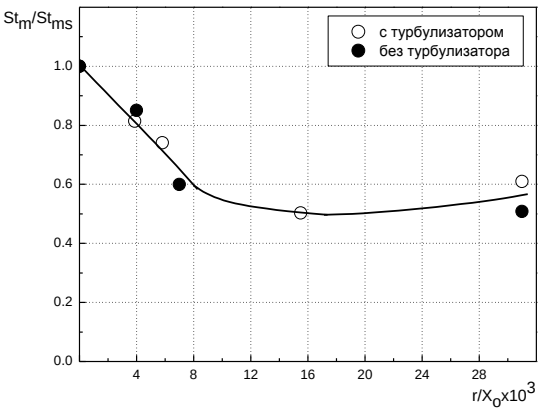

Fig. 6. Relative value of maximum Stanton number close to wedge with angle $\theta = 15°$ versus plate bluntness radius ($x/Xo = 0.64$, $M = 6$, $Re_{\infty L} = 19\times10^6$): 1-with turbulator, 2 – without turbulator [5].

5 Conclusion

Experimental and numerical investigations of entropy layer, generated by blunted leading edge of the plate, influence on flow in zone of oblique shock, generated close to wedge, interaction with turbulent boundary layer of the plate at Mach numbers $M_\infty = 5$ and 6 and Reynolds numbers up to 27×10^6 were carried out. Following results were obtained:

Small plate bluntness considerably reduces maximum values of dimensionless heat transfer coefficient (St_m) and pressure coefficient (Cp_m) in interference zone. At the same time zone of enhanced heat exchange and increased pressure slightly widens.

With increasing of plate bluntness radius r significant decrease of St_m occurs only up to some value of r, depending on parameters of incident flow, and further increase of bluntness radius weakly influences on St_m value. With increase of plate bluntness radius initial interference zone, preceding of quasi-conical interference zone, lengthens.

Plate bluntness at turbulent state of boundary layer gives rise to approximately the same heat transfer weakening in zone of shock incidence, as at transitional state of boundary layer before the shock (at the same values of M_∞ and $Re_{\infty L}$).

Results of numerical simulation of interference flow, fulfilled by means of solving Reynolds-averaged Navier-Stokes equations with use of q-ω turbulence model, at turbulence parameters chosen satisfactory agree with experimental data.

This work was fulfilled with financial support from RFBR (project no. 11-08-01099)

References

[1] Miller D.S., Hijman R., Redeker E., Janssen W.C., Mullen C.R. *A study of shock impingement on boundary layer at Mach 16*. Heat Transfer and Fluid

Mechanics Institute. Stanford, Calif.: Univ. Press, 1962. pp. 255 - 278

[2] Knight D., Yan H., Panaras A.G., Zheltovodov A. Advances in CFD prediction of shock wave turbulent boundary layer interactions. *Progr. in Aerospace Sci.*, Vol. 39, No. 2-3, pp. 121 – 184, 2003.

[3] Borovoy V. Ya., Egorov I. V., Skuratov A. S., Struminskaya I. V. Two-dimensional interaction of the oblique shock wave with the boundary and high-entropy layers of the blunt plate. AIAA 2011-731. 2011.

[4] Borovoy V., Mosharov V., Radchenko V. and Noev A. Laminar-turbulent flow around a fin placed on sharp and blunted plates. *EUCASS* 2009.

[5] Боровой В.Я., Мошаров В.Е., Радченко В.Н., Ноев А.Ю. Ламинарно-турбулентное течение вблизи клина, установленного на острой и затупленных пластинах. *Изв. РАН. МЖГ*, No. 3,. pp. 58 – 74, 2009.

[6] Боровой В.Я., Егоров И.В., Скуратов А.С., Струминская И.В. Взаимодействие косого скачка уплотнения с пограничным и высокоэнтропийным слоями плоской пластины. *Изв. РАН. МЖГ*, No. 6, pp. 89 – 108, 2005.

[7] Мошаров В.Е., Радченко В.Н. Новый метод визуализации течений на поверхности аэродинамических моделей. *Датчики и системы*, No. 5, pp. 48 – 53, 2010.

[8] Driscoll T.A., Vavasis S.A. Numerical conformal mapping using cross-ratios and Delaunay triangulation. *SIAM Journal. Sci. Comput*, Vol. 19, No. 6, pp. 1783–1803, 1998.

[9] Боровой В.Я., Егоров И.В., Ноев А.Ю., Скуратов А.С., Струминская И.В. Двумерное взаимодействие падающего скачка уплотнения с турбулентным пограничным слоем в присутствии энтропийного слоя. *Изв. РАН. МЖГ*, No. 6, pp. 76-97, 2011.

[10] *Основы теплопередачи в авиационной и ракетно-космической технике*. Под ред. В.К. Кошкина. М.: Машиностроение, 1975. 623с.

Copyright Statement